Advancements in precast concrete sandwich panels for load bearing structures

Pushpender Kumar [a,b,1], Nikhil Sanjay Nighot [c,d,2], Rajesh Kumar [e,3,*] , Surabhi Sharma [b,4], MS Kirgiz [f,g,5], Arpit Goyal [h,6]

[a] CSIR- Central Building Research Institute Roorkee, Uttarakhand, 247667, India
[b] Department of Civil Engineering, Jawaharlal Nehru Government Engineering College, Sundernagar, Himachal Pradesh, 175018, India
[c] PhD CSIR- Central Building Research Institute Roorkee, Uttarakhand, 247667, India
[d] Academy of Scientific and Innovative Research [AcSIR], Ghaziabad, 201002, India
[e] Senior Scientist, ACSC division, CSIR-CBRI Roorkee, Uttarakhand, 247667, India
[f] Department of Civil Engineering, Faculty of Engineering and Architectures, T.R. Istanbul Gelisim University, Avcilar, Istanbul 34310, Turkey
[g] Northwestern University, Chicago, IL 60208, USA
[h] Thapar Institute of Engineering and Technology, Patiala, Punjab, 147 004, India
[1] pushpender8698@gmail.com; [2] nikhilnighot1@gmail.com; [3] rajeshkumar@cbri.res.in; [4] sharma.surabhi07@gmail.com; [5] nakres42@yahoo.com; [6] arpit.goyal@thapar.edu
* corresponding author

ARTICLE INFO

Article history
Received April 17, 2024
Revised April 21, 2024
Accepted April 24, 2024
Available online April 27, 2024

Keywords
Precast concrete sandwich panel
Thermal insulation
Stone waste
Basalt fiber reinforced polyme
Axial test

ABSTRACT

Concrete sandwich panels consist of two concrete layers separated by an insulating foam core, offering thermal insulation, structural strength, and fire resistance. This study investigates sustainable precast concrete sandwich panels made with industrial waste materials like limestone slurry, quarry waste, and basalt fiber as shear connectors. The research evaluates the flexural and axial strength behavior of these panels and explores strategies to improve their structural performance. The panels were fabricated with outer concrete layers, an expanded polystyrene (EPS) insulation core, and basalt fiber connectors. Flexural tests using four-point bending and axial compression tests were conducted on panels with varying concrete layer thicknesses and basalt fiber widths. Findings revealed panels with thicker outer concrete layers (35mm) and wider basalt fiber connectors (11.5mm) exhibited higher cracking loads, load-hardening behavior, and increased ductility compared to thinner layers and narrower connectors. The axial test showed premature failure at the top and bottom quarters. Thicker concrete layers and wider basalt fiber connectors enhanced crack control, load distribution, and ductile behavior under flexural loading. Strengthening measures like additional reinforcement, proper anchorage detailing, and increased shear reinforcement at the end regions are recommended to improve axial load-bearing capacity and prevent premature end failures. The PCSP demonstrated up to 40% cost savings over commercial products while providing better thermal insulation than conventional brick masonry due to the EPS core. Overall, the study promotes developing sustainable, energy-efficient, and cost-effective load-bearing sandwich panel systems.

1. Introduction

A concrete sandwich panel is a composite building material made up of two exterior layers of concrete separated by an insulating foam core [1]. These panels, sometimes called structural insulated panels (SIPs), have significant advantages over traditional construction methods. First and foremost, the insulating foam core provides excellent thermal insulation, lowering energy expenses for heating and cooling the structure [2], [3]. Second, the concrete layers contribute to total structural strength, making these panels acceptable for load-bearing applications while being fire-resistant due to the concrete's non-combustible nature.

Despite the use of concrete, the panels' overall weight is very modest due to the lightweight insulating foam core, making them easy to handle and install [4]. While concrete sandwich panels are more expensive than other traditional construction methods, their numerous benefits, including energy efficiency, durability, and versatility, make them an appealing choice for a wide range of construction projects [5].

Rajasthan holds the largest share in the Indian stone industry, with abundant reserves of marble, sandstone, granite, and limestone that significantly boost the state's economy. However, the mining of Kota stone in the region has raised environmental concerns due to the substantial disposal of solid and slurry waste. Approximately 10 million tons of waste are generated annually from cutting and polishing Kota stone [6]. Data indicates that 42% of the raw mined stone is transformed into finished products, while the remaining 58% is categorized as waste, comprising 30% mining waste, 17% dressing waste, and 11% polishing waste [7]. This large accumulation of waste is utilized to create concrete sandwich panels, promoting sustainability and reducing pollution.

The paper examines the flexural and axial strength behavior of precast concrete sandwich panels made by mixing low-grade limestone slurry, and quarry waste with concrete, and incorporating basalt fiber as a shear connector and expanded polystyrene (EPS) as the insulation layer. Limestone slurry and quarry waste were likely used as supplementary cementitious materials to reduce the overall cost of the concrete mixture and potentially improve its durability and workability [8]–[10]. Incorporating industrial by-products or waste materials in concrete is a sustainable approach that reduces the environmental impact of construction activities. Basalt fiber was chosen as a shear connector instead of traditional steel connectors due to its lower thermal conductivity, which helps reduce thermal bridging through the panel [11], [12]. Thermal bridging is a phenomenon where heat is easily transferred through materials with high thermal conductivity, resulting in higher energy consumption for heating and cooling. Additionally, basalt fiber offers high tensile strength while being relatively inexpensive compared to other fiber reinforcements. EPS was used as the insulation layer in the panel to provide better thermal insulation and improve the overall energy efficiency of the structure. EPS is a lightweight, cost-effective, and widely available insulation material with good thermal resistance properties [13], [14].

The four-point bending test was performed to evaluate the panel's performance under failure conditions and determine whether the PCSP can attain the necessary bearing capacity to withstand flexural and axial loads. This test is crucial for ensuring the structural integrity and safety of the proposed panel design. Overall, the choice of materials and the structural testing aim to develop a more sustainable, energy-efficient, and cost-effective precast concrete sandwich panel system while maintaining the required structural performance.

2. Method

2.1. Characterization of raw materials

Cement: Ordinary Portland cement (OPC)-43 grade, per IS:8112-2013 [15], was obtained from M/s Ultratech Cement Ltd., India, and used as the main binder for the concrete mix. Typically, the cementitious content lies between 300kg/m3 and 400 kg/m3, although up to 500 kg/m3 has been used in the presented research. The cement's chemical composition was examined by IS 4032, given in Table 1 which confirms IS:8112-1989 [16]. The results in Table 1 show that calcium oxide (CaO) and tricalcium silicate (C3S) were the major oxides present in the OPC binder.

Table 1. XRF analysis of cement

Chemical composition	Percentage [%]
CaO	64.34
SiO_2	18.83
Al_2O_3	05.93
Fe_2O_3	05.52
MgO	00.91
SO_3	02.28
K_2O+TiO_2	01.76
C_3S	64.84
C_2S	18.35
C_3A	08.96
C_4AF	05.75

- Fly ash

  Fly ash conforming with IS 3812 (Part 1):2003 [17] and complying with ASTM standard C618 [18] was employed in this experiment. Fly ash of the Class F [siliceous kind] with a high alumina concentration has been used. It was found that fly ash [D50= 19.40µm] had smaller particles than cement. The particle size distribution of fly ash was determined using a Horiba Laser particle size analyzer as shown in Table 2. Moreover, XRD enables the precise identification of different phases in anhydrous cementitious materials. From the results in Table 2, it can be observed that silica was the major oxides present in the fly ash.

Table 2. Chemical composition of fly ash

Chemical composition	SiO2	Al2O3	Fe2O3	CaO	MgO	SO3	Loss on ignition	Free CaO
Percentage [%]	63.21	27.65	5.24	1.46	0.83	0.40	0.60	-

- Fine aggregate

  The fine aggregate used in this investigation was local river sand of a very fine grade collected from a nearby location in Solani River, Roorkee. The river sand specifications conformed to the Indian Standard BIS:383 [19]. The fineness modulus of the sand was 1.13, indicating a very fine gradation. The sand was required to pass through a 4.75 mm I.S. sieve. Before use, the sand was surface-dried to allow for proper moisture content control when batching concrete mixes. Utilizing natural river sand from local sources as the fine aggregate is a common practice, and characterizing its properties like gradation and conformance to standards is important for concrete mix design and performance evaluations.

- Low-grade limestone slurry

Low-grade limestone slurry (LgLS) was collected from the polishing and cutting plants of the Indraprasth industrial sector in Kota, Rajasthan. After being crushed and allowed to dry in an open environment, a chemical analysis was performed in preparation for more studies. The XRF-Analysis was conducted to determine the chemical composition of the limestone slurry as shown in Table 3. This analysis helps in understanding the elemental composition of the limestone sample, providing valuable insights for further studies.

Table 3. XRF analysis of LgLS

Chemical Composition	CaO	SiO2	MgO	Fe2O3	Al2O3	K2O+TiO2	P2O5	SO3
Percentage [%]	36.85	23.51	00.84	02.63	02.61	01.46	0.89	0.26

- Stone waste aggregate

Kota stone, which is a stone quarry waste, has been added to the concrete mix. Kota stone is a fine-grained limestone, obtained from different quarry sites of Rajasthan. Kota stone slurry, ranging from a few micrometers to around 0.075 mm, was employed as a fine filler and for cement-based products. Kota stone fine aggregate, with particle sizes between 0.075 mm and 4.75 mm, was used in concrete mixes and mortars, providing strength and workability. For the coarse aggregate requirements, Kota stone aggregate, with sizes from 4.75 mm to 20 mm, was incorporated into concrete as shown in Fig. 1.

Fig. 1. Different sizes of Kota stone waste

- Expanded polystyrene EPS

The EPS sheet purchased from the market underwent a series of tests at the laboratory of CSIR-CBRI, following the guidelines outlined in the relevant Indian Standard codes. The bulk density test, conducted as per IS 5688: 1984, yielded a result of 28 kg/m³, exceeding the minimum requirement of 15 kg/m³. The compressive strength test at 10% strain, performed according to IS 4671: 1984 [20], showed a value of 0.50 MPa, which surpassed the minimum criterion of 0.14 MPa. Additionally, the cross-breaking strength test, also following IS 4671: 1984, resulted in a value of 0.90 MPa, well above the minimum requirement of 0.22 MPa. Consequently, the EPS sheet successfully met all the specified criteria for the respective tests, demonstrating its compliance with the relevant Indian Standard codes.

- Basalt fiber connector

Basalt fiber has been seen as a competent replacement for traditionally used fibers like glass, carbon, and aramid due to its outstanding characteristics. One of its top points which is really worth mentioning is its amazing strength-to-weight ratio, which means that it is lightweight but extremely strong and therefore suitable for construction and automotive industries demanding high tensile strength [21]. Basalt fiber also shows excellent resistance to temperature and chemicals, in which it can bear temperatures up to 800°C (1472°F) and is resistant to various harsh chemicals, therefore, it is fit for harsh environments or fire-resistant applications [22]. The fiber can be obtained from basalt rock and it is not only environmentally friendly but also non-corrosive and non-toxic, which is safer and has a lower environmental impact than synthetic fibers. Besides, basalt fiber even has insulation features and is used for soundproofing and heat insulation, for example, in buildings as well as in noise reduction. Its robustness against moisture, alkalis, and acids, besides its ability to survive in demanding conditions like reinforced concrete structures and chemical storage tanks [23], makes it a long-lasting and reliable choice. Although at times it may cost more than some fibers, basalt fiber's outstanding properties and long lifespan usually make it the cheapest alternative over a longer term [24].

- Concrete mix and Casting procedure

The casting of the panel was made considering variables such as the outer concrete thickness and the width/thickness of the basalt polymer connectors. Core thicknesses of 70 mm were selected to meet the U-value criteria for Energy Conservation Building Codes [25]. The concrete mix proportion [26], [27] consisted of OPC, sand, and aggregate in a ratio of 1:1.03:1.7, with a water-binder ratio of 0.96. Basalt fiber grids sized 20 × 20 mm served as shear connectors between the concrete skins, while the coarse aggregate particle size ranged from 4.75 to 20 mm.

The process involved preparing an EPS sheet to the required dimensions and passing the basalt fiber connectors through it, ensuring equal spacing on both sides. A steel mold with inner dimensions of 1000 × 500 × 140 mm was utilized. After placing proper support in the mold, the EPS sheet with basalt fiber connectors was positioned and fixed. Concreting was done on one side of the panel initially, followed by concreting on the other side after 24 hours. The panel specimens were then cured for 28 days

3. Results and Discussion

3.1. Flexural test

In a flexural test for concrete sandwich panels, the panels are subjected to bending forces to assess their structural performance and load-bearing capacity as shown in Fig. 2. This test involves incrementally applying a load to the center of the panel until it reaches failure or a predetermined limit. Throughout the test, measurements are taken to evaluate parameters like deflection, ultimate load, and stress distribution. Flexural tests were conducted on concrete sandwich panels with different widths of the basalt fiber and different outer concrete wythe.

The specimen dimensions for the test were 1000 × 500 × 140 mm. The test setup for four-point bending involved simply supported boundary conditions. In the four-point bending tests, the point loading was transferred to the specimens using a hydraulic jack and distributed through a rigid steel girder and two solid steel round bars across the width of the panels to produce two-line loads. Fig. 3 showcases different sample configurations for evaluating the use of geogrids as reinforcement in concrete structures. Geogrids are grid-like geosynthetic materials made of polymers, designed to provide tensile reinforcement when embedded in soil or concrete.

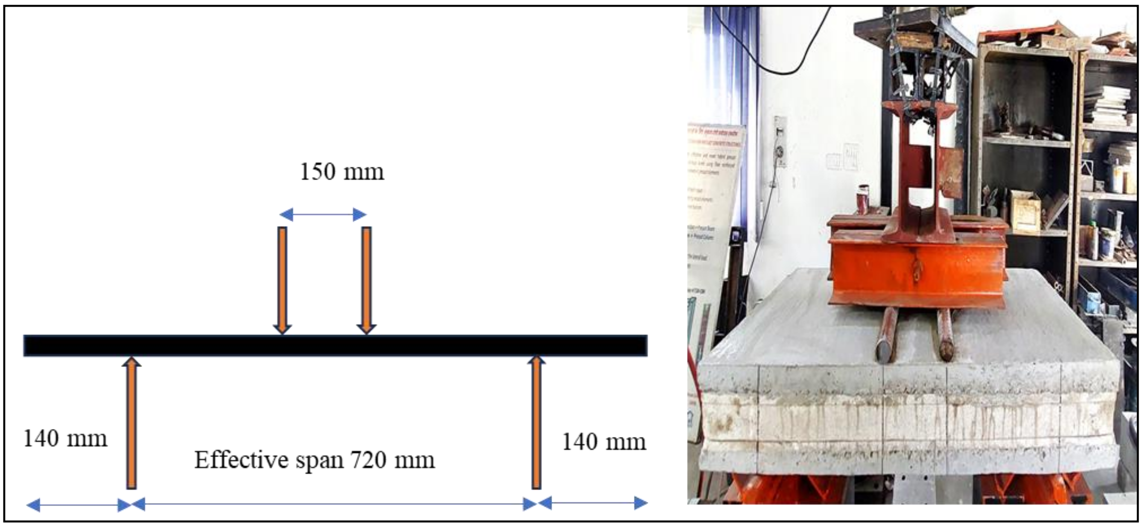

Fig. 2. Free body diagram and Setup used for of 4-point bending test

In the Fig. 3, the measurements of 7.5 mm and 11.5 mm refer to the width or thickness of the geogrid reinforcement being used. For the 7.5 mm geogrid, two different concrete cover thicknesses are being tested – one with 20 mm of concrete covering the geogrid on one side, and another with 50 mm of concrete cover on one side. This variation in concrete cover thickness can impact the performance and durability of the geogrid reinforcement, as the concrete cover plays a crucial role in protecting the geogrid from environmental exposure and providing a strong bond between the materials. In contrast, for the 11.5 mm geogrid, a consistent concrete cover thickness of 35 mm is maintained on both sides. This consistency allows for a controlled comparison of the 11.5 mm geogrid's performance under uniform concrete cover conditions.

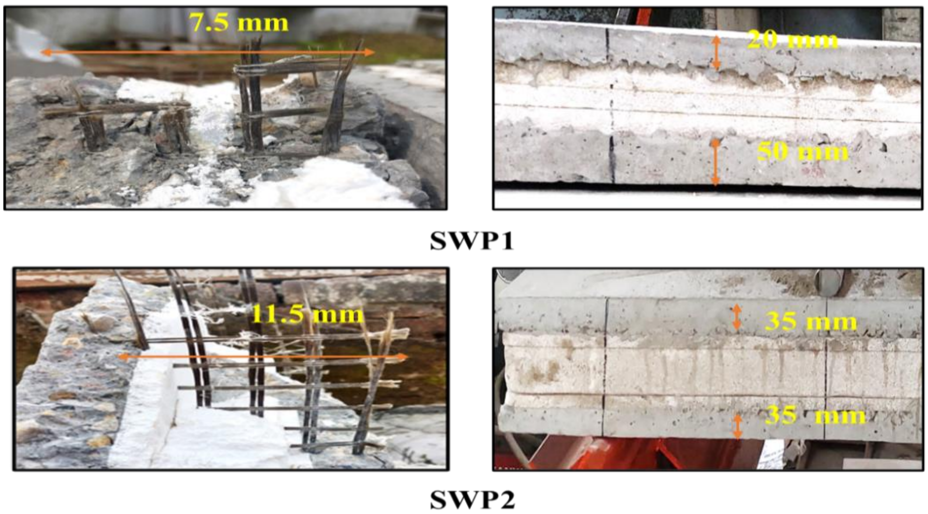

Fig. 3. Panel configuration

The varying concrete cover thicknesses and geogrid widths are commonly conducted to assess the optimal combination of geogrid dimensions and concrete cover thicknesses for specific structural applications, taking into account factors such as load-bearing capacity, durability, and cost-effectiveness.

3.2. Cracking Pattern and Failure Mode

The images show the cracking patterns and failure modes of two types of sandwich wall panels (SWPs) after undergoing flexural tests (Fig. 4). SWP1, with a thinner outer concrete layer ranging from 20mm to 50mm and a narrower 7.5mm geogrid width, exhibited a distinct failure behavior compared to SWP2, which had a constant 35mm outer concrete thickness and a wider 35mm geogrid. Fig. 4 represents different flexural failure of the panel.

For SWP1, the initial crack rapidly propagated into a penetrating crack spanning the entire width of the panel's bottom concrete layer [wythe]. This rapid and extensive crack development indicates that the thin outer concrete layers and narrow geogrid width were unable to effectively resist and distribute the applied flexural load, resulting in a brittle and sudden failure mode. The crack opening appears to have widened significantly after initiation, further highlighting the lack of crack control and load-carrying capacity in this panel configuration.

In contrast, SWP2 exhibited a more gradual and controlled cracking pattern. Multiple microcracks initiated in the bottom wythe and gradually propagated upwards as the flexural load increased. Earlier, cracks appeared narrower and more distributed compared to SWP1, suggesting improved crack resistance and load distribution capabilities. One of the images reveals a significant increase in crack width when the cracks reached the upper concrete layer, potentially indicating delamination or loss of composite action between the layers at higher load levels.

The distinct differences in cracking patterns and failure modes can be attributed to the variations in concrete layer thicknesses and geogrid widths between the two-panel types. The constant 35mm outer concrete thickness and wider 11.5mm geogrid in SWP2 contributed to enhanced crack control and a more ductile failure behavior compared to the sudden, brittle failure observed in SWP1 with the thinner layers and narrower geogrid.

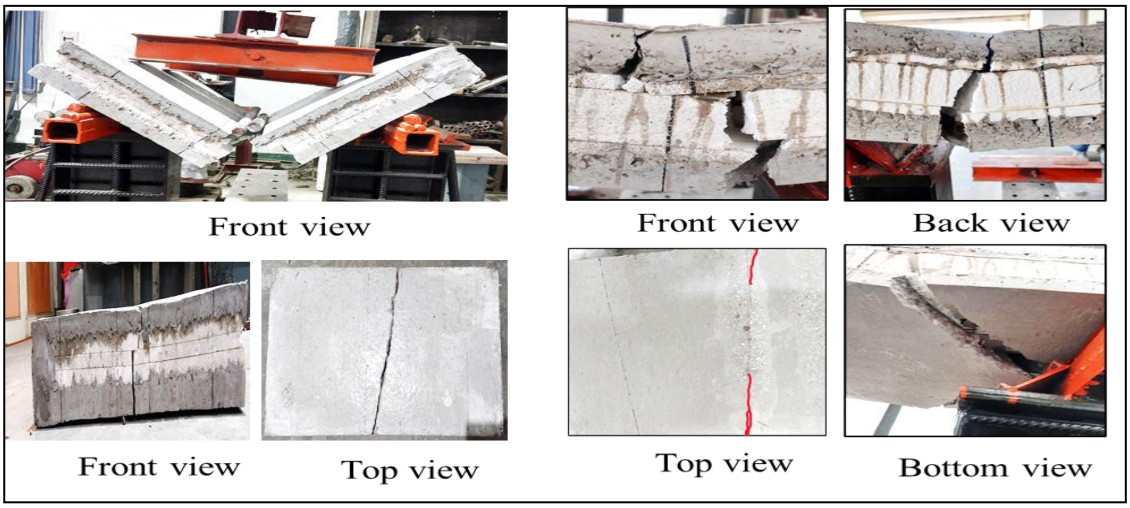

Fig. 4. Different flexural failure

3.3. Load-Deflection Response

The load-deflection response of the sandwich wall panels provides valuable insights into their structural behavior under flexural loading as shown in Fig. 5. The cracking load, which is the load at which the first visible crack forms in the panel, was higher for SWP2 compared to SWP1. This can be attributed to the higher cracking strain of SWP2 compared to SWP1. The higher cracking strain enabled SWP2 to resist greater loads before the initial crack formation.

The ductility behavior of the panels is quantified by the ductility index [μ], defined as the ratio of ultimate deflection to yield deflection [$\mu = \delta u/\delta y$]. Higher values of μ indicate more ductile behavior, which is desirable for structural safety and resilience. SWP2 exhibited higher ductility index values compared to SWP1, signifying a more ductile failure mode. The enhanced ductility of SWP2 can be attributed to the thicker concrete layers and wider geogrid, enabling better load redistribution and controlled cracking patterns. Overall, the thicker concrete layers and wider geogrid in SWP2 resulted in a higher cracking load, load-hardening behavior after cracking, and increased ductility compared to SWP1. These characteristics contribute to improved structural performance and failure resistance under flexural loading conditions, making SWP2 a more desirable configuration for sandwich wall panel design and application.

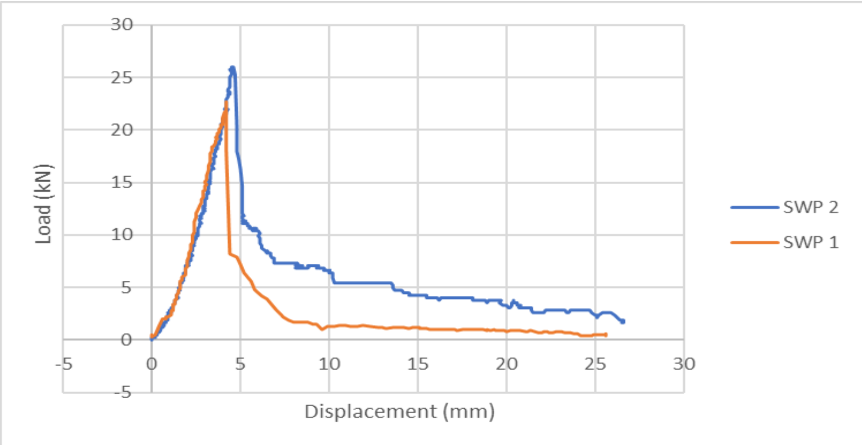

Fig. 5. Load vs Displacement graph for SWP1 and SWP2

3.4. Axial test

Axial tests on concrete sandwich panels are typically performed to evaluate the axial load-bearing capacity and behavior of these composite structural elements. The axial test setup typically involves applying a compressive axial load along the length of the sandwich panel specimen as shown in Fig. 6. The specimen is placed between two loading platens or anchorage systems that ensure uniform load distribution and prevent premature failure due to stress concentrations.

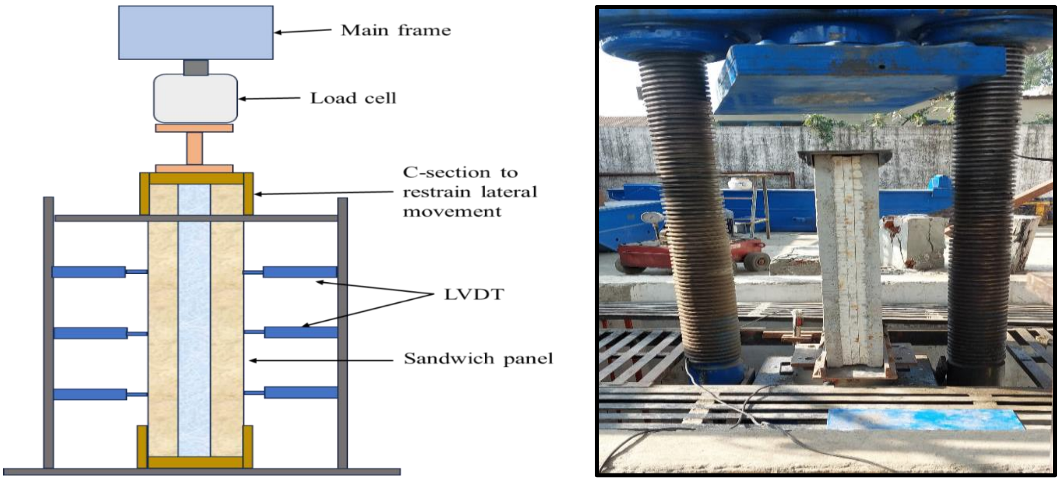

Fig. 6. Set up of axial load test

The panel under investigation experienced a maximum peak load of 419 kN at a displacement of 13.32 mm as shown in Fig. 7. However, the failure of the panel occurred only at the top and bottom quarters as shown in Fig. 8, which constitute one-fourth of the panel's length from each end. Interestingly, no signs of cracking or failure were visible in the middle portion of the panel.

This observation indicates that the panel needs to be strengthened at the end portions to ensure that the axial load is properly transferred through the entire length of the panel.

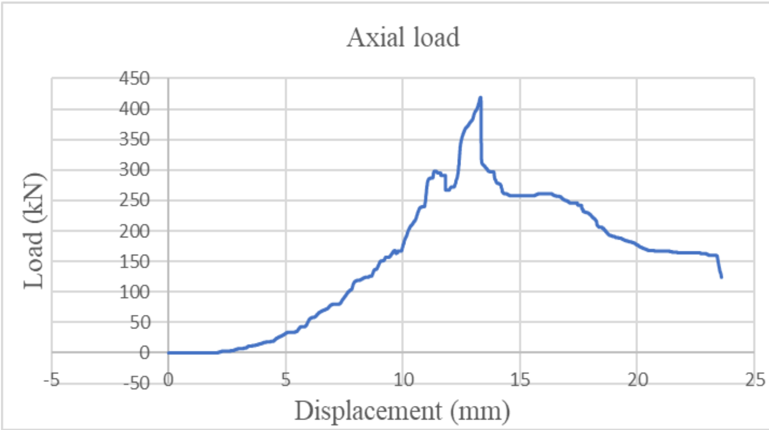

Fig. 7. Load deflection curve for axial test

To address this issue, several strengthening measures can be implemented. Firstly, additional reinforcement, such as more steel bars, higher-strength concrete, or external fiber-reinforced polymer wraps, can be provided at the top and bottom quarters of the panel. This will increase the load-carrying capacity and ductility of the end regions. Secondly, proper anchorage detailing of the reinforcement bars should be ensured at the end regions to prevent premature pullout or bond failures. Thirdly, adequate confinement reinforcement, such as closely spaced ties or spirals, can be installed at the end regions to enhance the confinement of the concrete and prevent premature spalling or crushing. Fourthly, increasing the shear reinforcement, such as stirrups or bent bars, at the end regions can help resist the higher shear stresses expected in those areas. By implementing one or more of these strengthening measures at the end portions of the panel, the overall load distribution can be improved, enabling the panel to resist higher axial loads without premature failure at the ends. Fig. 8(b) represents the better bond strength between the concrete and EPS sheet even after 1 year later of testing.

(a) Front view (b) Sample extracted Adhesive bond

Fig. 8. Failure of axial test

3.5. Comparison with conventional panels

The Table 4 presents a comparison between a CBRI Sandwich Panel and conventional panels across several parameters. The density of the CBRI Sandwich Panel is given as nearly 1400 kg/m3. Its cost is stated to be 40% less than a commercial product, with the remark that waste aggregate is used, which likely contributing to the cost savings. The dead weight of the panel is significantly lower than conventional brick masonry, with the remark identifying it as a lightweight panel having a density lesser than 2000 kg/m3. In terms of thermal insulation, the CBRI Sandwich Panel performs better than brick masonry.

Table 4. Comparison between a CBRI Sandwich Panel and conventional panels

Parameter	CBRI Sandwich Panel	Remarks
Density	Nearby 1400 kg/m3	-
Cost	-40% less than commercial product	Waste aggregate is used
Dead Weight	Significantly lower than conventional brick masonry	Lightweight panel as having a density lesser than 2000 kg/m3
Thermal Insulation	Better than brick masonry	EPS core provides insulation

4. Conclusion

The use of precast composite wall panels can facilitate faster construction. Therefore, in the presented study; the experimental study examined the structural performance of sandwich wall panels with different configurations. Based on the conducted experiments; the following observations have been made. 1) Sandwich wall panels with thicker outer concrete layers (35mm) and wider geogrid reinforcement (11.5mm) exhibited improved structural performance compared to panels with thinner layers (20-50mm) and narrower geogrid (7.5mm); 2) The thicker and wider reinforced SWP2 showed higher cracking loads, load-hardening behavior after cracking, and increased ductility compared to the thinner SWP1; 3) The axial load test revealed that the panel experienced premature failure at the top and bottom quarters, while the middle portion remained intact; 4) To improve the axial load-bearing capacity and prevent premature end failures, several strengthening measures are recommended: a. Additional reinforcement at the end regions [steel bars, higher-strength concrete, FRP wraps]. b. Proper anchorage detailing and confinement reinforcement at the ends. c. Increased shear reinforcement at the end regions.

Acknowledgment

The authors are thankful to the Director, CSIR- Central Building Research Institute.

Declarations

Author contribution. All authors contributed equally to the main contributor to this paper. All authors read and approved the final paper
Funding statement. None of the authors have received any funding or grants from any institution or funding body for the research.
Conflict of interest. The author is grateful to 'The Ministry of Environment, Forest and Climate Change [MoEF & CC], New Delhi, Government of India' for the sustained financial support to the project [File Number: 19/45/2018/RE; Project No.: GAP-0120]..
Additional information. No additional information is available for this paper.

References

[1] T. Zheng, Q. Ge, F. Xiong, G. Li, Y. Xue, and X. Deng, "Study of the flexural performance and a novel calculation formula for the degree of composite action for precast concrete sandwich panels," Struct. Des. Tall Spec. Build., vol. 32, no. 18, p. e2065, Dec. 2023, doi: 10.1002/tal.2065.

[2] Q. Tushar, G. Zhang, M. A. Bhuiyan, S. Navaratnam, F. Giustozzi, and L. Hou, "Retrofit of Building Façade Using Precast Sandwich Panel: An Integrated Thermal and Environmental Assessment on BIM-Based LCA," Buildings, vol. 12, no. 12, p. 2098, Nov. 2022, doi: 10.3390/buildings12122098.

[3] Q. Huang, E. Hamed, and R. I. Gilbert, "Early-Age Shrinkage Effects in Precast Concrete Sandwich Panels," PCI J., vol. 65, no. 1, pp. 74–88, 2020, doi: 10.15554/pcij65.1-04.

[4] Kamale G and Satheesh Kumar K R P, "Analytical Study on Profiled Steel Sheet – Concrete Composite Sandwich Panel under Axial Load," Int. J. Adv. Res. Sci. Commun. Technol., pp. 371–376, Jun. 2022, doi: 10.48175/IJARSCT-4825.

[5] F. H. Fouad, J. Farrell, M. Heath, A. Shalaby, and A. Vichare, "Behavior of the MR Sandwich Panel in Flexure," in SP-260: Fabrication Technology for Thin Cementitious Products, Jun. 2009, vol. 260, pp. 73–88, doi: 10.14359/56626.

[6] A. Kumar and S. Chaudhuri, "Improving Urban Air Quality Monitoring in Delhi, India: Reflections on Low-Cost Air Quality Sensors (LCAQS) and Participatory Engagement," Environ. Urban. ASIA, vol. 13, no. 2, pp. 265–283, Sep. 2022, doi: 10.1177/09754253221122752.

[7] D. G. (Haryana) Mines and Geology Department, "District Survey Report (Mining)," 2021. [Online]. Available at: https://mines.rajasthan.gov.in/dmgcms/Static/files/DSR Udaipur 2024 for All Minerals 30.04.2024.pdf.

[8] D. Wang and H. Jia, "A quantitative study on the synergistic effect between limestone powder and supplementary cementitious materials," Adv. Cem. Res., vol. 34, no. 7, pp. 324–330, Jul. 2022, doi: 10.1680/jadcr.21.00027.

[9] I. Bhandari, R. Kumar, A. Sofi, and N. S. Nighot, "A systematic study on sustainable low carbon cement – Superplasticizer interaction: Fresh, mechanical, microstructural and durability characteristics," Heliyon, vol. 9, no. 9, p. e19176, Sep. 2023, doi: 10.1016/j.heliyon.2023.e19176.

[10] N. S. Nighot and R. Kumar, "A comprehensive study on the synthesis and characterization of eco-cementitious binders using different kind of industrial wastes for sustainable development," Dev. Built Environ., vol. 14, p. 100135, Apr. 2023, doi: 10.1016/j.dibe.2023.100135.

[11] J. Huang, Q. Jiang, X. Chong, X. Ye, and C. Liu, "Structural performance of a façade precast concrete sandwich panel enabled by a bar-type basalt fiber-reinforced polymer connector," Front. Struct. Civ. Eng., vol. 17, no. 1, pp. 122–137, Jan. 2023, doi: 10.1007/s11709-022-0894-1.

[12] S. Fang, W. Xiao, K. Chen, and X. Song, "Study on the thermal decay mechanism of basalt fiber reinforced resin based friction materials," Ind. Lubr. Tribol., vol. 75, no. 10, pp. 1236–1245, Nov. 2023, doi: 10.1108/ILT-07-2023-0233.

[13] M. Harit and K. Kumar, "A Critical Review of Expanded Polystyrene Core Panel System in Buildings in India," J. Sustain. Constr. Eng. Proj. Manag., vol. 4, no. 3, pp. 1–7, 2022. [Online]. Available at: https://zenodo.org/records/5891721.

[14] A. H. S. Ragab, E. M. E. Attiah, M. A. Shebl, and A. A. H. Nasser, "Comparative analysis of thermal performance for precast panel systems with conventional and innovative insulation materials," HBRC J., vol. 19, no. 1, pp. 427–452, Dec. 2023, doi: 10.1080/16874048.2023.2283294.

[15] Bureau of Indian Standard(BIS), "IS: 8112 – 1989, Specification for 43 grade Ordinary Portland Cement," 2013. [Online]. Available at: https://law.resource.org/pub/in/bis/S03/is.8112.1989.pdf.

[16] "IS 8112: Specification for 43 grade ordinary Portland cement," Bureau of Indian Standards, 1989. [Online]. Available at: https://archive.org/details/gov.in.is.8112.1989.

[17] IS:3812 (Part-1), "Pulverized fuel ash — specification. Part 1: For use as Pozzolana in cement, Cement Mortar and Concrete (Second Revision)," Bur. Indian Stand. New Delhi, India, no. October, pp. 1–14, 2013, [Online]. Available at: https://law.resource.org/pub/in/bis/S03/is.3812.1.2003.pdf.

[18] "C618 Standard Specification for Coal Fly Ash and Raw or Calcined Natural Pozzolan for Use in Concrete," ASTM International, 2023. [Online]. Available at: https://www.astm.org/c0618-22.html.

[19] IS 2386 (part III), "Method of Test for aggregate for concrete. Part III- Specific gravity, density, voids, absorption and bulking," Indian Stand., vol. 2014, p. (Reaffirmed 2002), 1970, [Online]. Available at: https://apps.crossref.org/SimpleTextQuery.

[20] Bureau of Indian Standards, "IS 4671: 1984 Specifications for expanded polystyrene for thermal insulation purposes," 1984. [Online]. Available at: https://archive.org/details/gov.in.is.4671.1984/page/n21/mode/2up.

[21] B. N. Al-Kharabsheh et al., "Basalt Fiber Reinforced Concrete: A Compressive Review on Durability Aspects," Materials (Basel)., vol. 16, no. 1, p. 429, Jan. 2023, doi: 10.3390/ma16010429.

[22] A. Qsymah et al., "Thermal properties, microstructure analysis, and environmental benefits of basalt fiber reinforced concrete," J. Eng. Fiber. Fabr., vol. 18, p. 155892502211465, Jan. 2023, doi: 10.1177/15589250221146547.

[23] Z. Xue, P. Qi, Z. Yan, Q. Pei, J. Zhong, and Q. Zhan, "Mechanical Properties and Crack Resistance of Basalt Fiber Self-Compacting High Strength Concrete: An Experimental Study," Materials (Basel)., vol. 16, no. 12, p. 4374, Jun. 2023, doi: 10.3390/ma16124374.

[24] A. R. Tavadi, Y. Naik, K. Kumaresan, N. I. Jamadar, and C. Rajaravi, "Basalt fiber and its composite manufacturing and applications: An overview," Int. J. Eng. Sci. Technol., vol. 13, no. 4, pp. 50–56, May 2022, doi: 10.4314/ijest.v13i4.6.

[25] "Energy Conservation Building Code (ECBC)," *Bureau Of Energy Efficiency*, Government of India, Ministry of Power, 2017. [Online]. Available at: https://beeindia.gov.in/en/energy-conservation-building-code-ecbc.

[26] "IS 10262 : 2019: Concrete Mix Proportioning — Guidelines (Second Revision)," 2019. [Online]. Available at: https://archive.org/details/gov.in.is.10262.2019.

[27] "IS 456 Plain Concrete and Reinforced," *Bureau of Indian Standards, New Dehli* pp. 1-114, 2000. [Online]. Available at: https://law.resource.org/pub/in/bis/S03/is.456.2000.pdf.